

11 Top pair production and mass determination

Contribution* by: A. Maier [[andreas.martin.maier@desy](mailto:andreas.martin.maier@desy.it)]

The mass of the top quark can be measured in a well-defined scheme and with unrivalled precision at a future electron–positron collider, like the FCC-ee. The most sensitive observable is the total production cross-section for $b\bar{b}W^+W^-X$ final states near the top pair production threshold. I review the state of the art in theory predictions for this quantity.

11.1 Introduction

The total cross-section for inclusive $b\bar{b}W^+W^-X$ production can be measured with very high precision at a future high-energy electron–positron collider. Owing to the potential for large integrated luminosity, the FCC-ee is especially well-suited for such a measurement. The line shape for centre-of-mass energies close to the top–antitop production threshold is highly sensitive to the mass of the top quark, which allows its determination with unprecedented precision. Since the statistical uncertainty of the measurement is projected to be significantly below the current theory error [1, 2], it is crucial to continuously improve the theoretical prediction.

11.2 Effective theory framework

The $b\bar{b}W^+W^-X$ final state is mostly produced through the creation and decay of non-relativistic top–antitop pairs, interacting predominantly via a colour Coulomb potential. The dynamics of this system are described by potential non-relativistic effective field theory (PNREFT) [3–5], combined with unstable particle effective field theory [6, 7]. Within this framework, higher-order corrections can be treated systematically through a simultaneous expansion in the non-relativistic velocity v and the strong, electromagnetic, and top Yukawa couplings α_s , α , and y_t . We adopt the power counting $v \sim \alpha_s \sim \sqrt{\alpha} \sim y_t$ with the top quark width $\Gamma_t \sim m_t \alpha$. Powers of α_s/v from the bound-state interaction are resummed to all orders in perturbation theory.

At leading order, the PNREFT Lagrangian is given by

$$\mathcal{L}_{\text{PNREFT, LO}} = \psi^\dagger \left(i\partial_0 + \frac{\vec{\partial}^2 + im_t \Gamma_t}{2m_t} \right) \psi + \mathcal{L}_{\text{anti-quark}} - \int d^3\vec{r} [\psi^\dagger \psi](\vec{x} + \vec{r}) \frac{C_F \alpha_s}{r} [\chi^\dagger \chi](\vec{x}), \quad (11.1)$$

where ψ is the quark field and χ the antiquark field. The resulting top pair propagator is the Green function of the Schrödinger equation with the colour Coulomb potential interaction. Its imaginary part is closely related to the resonant top pair production cross-section via the optical theorem.

11.3 Higher-order corrections

Higher-order corrections to the PNREFT Lagrangian are obtained by matching to the full Standard Model. In the first step, hard modes with large four-momenta $k \sim m_t$ are integrated out. This gives rise to a non-relativistic effective field theory with local effective vertices. These

*This contribution should be cited as:

A. Maier, Top pair production and mass determination, DOI: [10.23731/CYRM-2020-003.117](https://doi.org/10.23731/CYRM-2020-003.117), in: Theory for the FCC-ee, Eds. A. Blondel, J. Gluza, S. Jadach, P. Janot and T. Riemann, CERN Yellow Reports: Monographs, CERN-2020-003, DOI: [10.23731/CYRM-2020-003](https://doi.org/10.23731/CYRM-2020-003), p. 117. © CERN, 2020. Published by CERN under the [Creative Commons Attribution 4.0 license](https://creativecommons.org/licenses/by/4.0/).

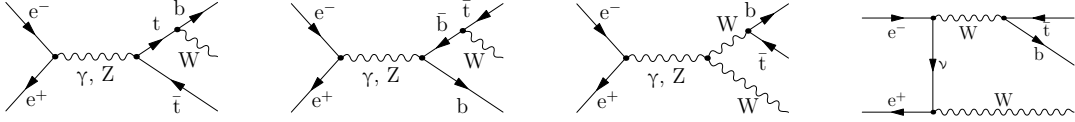


Fig. B.11.1: Non-resonant diagrams contributing to the $W^+b\bar{t}$ final state at NLO. The final state $W^-b\bar{t}$ follows from charge conjugation.

matching corrections are known to NNNLO in the QCD and Higgs sector [8–11] and to NNLO in the electroweak sector [12–16].

In the second matching step, soft modes $k \sim m_t v$ and potential modes $k_0 \sim m_t v^2, \vec{k} \sim m_t v$ for gluons and light quarks are also eliminated from the theory. The most challenging part is the calculation of the corrections to the static colour Coulomb potential to NNNLO, which is reported in Refs. [17–19].

11.3.1 Resonant production

With the matched PNREFT Lagrangian, the resonant top pair production cross-section can be calculated, including NNNLO QCD and Higgs effects and NNLO electroweak effects, by computing corrections to the Green function to this order. The complete result for the QCD corrections was first presented for the S-wave contribution in Ref. [20] and for the P-wave contribution in Ref. [9] (see also Ref. [21]). Schematically, the known contributions to the top pair production cross-section can be written as

$$\sigma_{\text{res}} \sim \alpha^2 v \sum_{k=0}^{\infty} \left(\frac{\alpha_s}{v} \right)^k \times \begin{cases} 1 & \text{LO} \\ \alpha_s, v, \frac{\alpha}{v} & \text{NLO} \\ \alpha_s^2, \alpha_s v, v^2, \frac{\alpha}{v} \times \left\{ \frac{\alpha}{v}, \alpha_s s, v \right\}, y_t \sqrt{\alpha}, y_t^2 & \text{NNLO} \\ \alpha_s^{3-i} v^i, y_t^2 \times \left\{ \frac{\alpha}{v}, \alpha_s, v \right\} & \text{NNNLO} \end{cases} \quad (11.2)$$

11.3.2 Non-resonant production

Top quarks are unstable and the final state $b\bar{b}W^+W^-X$ can also be produced in non-resonant channels that do not involve the creation of a top–antitop pair near the mass shell. According to unstable particle effective field theory, the full cross-section is given by the sum of the resonant and non-resonant contributions:

$$\sigma = \sigma_{\text{res}} + \sigma_{\text{non-res}} \quad (11.3)$$

While non-resonant production is suppressed by one power of α , it does not suffer from the same phase space suppression as resonant production and therefore contributes with a factor of α/v relative to the leading-order cross-section, i.e., at NLO. The diagrams at this order are shown in Fig. B.11.1; their contribution was first detailed in Ref. [22]. The NNLO non-resonant cross-section was later detailed in Ref. [16].

Virtual top quarks in the non-resonant channels are formally far off-shell with squared momenta $p_t^2 - m_t^2 \sim m_t^2 \gg m_t \Gamma_t$, so the width must not be resummed in the propagators. Since we integrate over the full phase space, endpoint divergences occur whenever $p_t^2 - m_t^2$ vanishes. At NNLO, this leads to poles proportional to Γ_t/ϵ in $4 - 2\epsilon$ dimensions. As usual in asymptotic expansions, these cancel against poles in a different expansion region. In this case, the corresponding poles appear in the form of finite-width divergences in the resonant

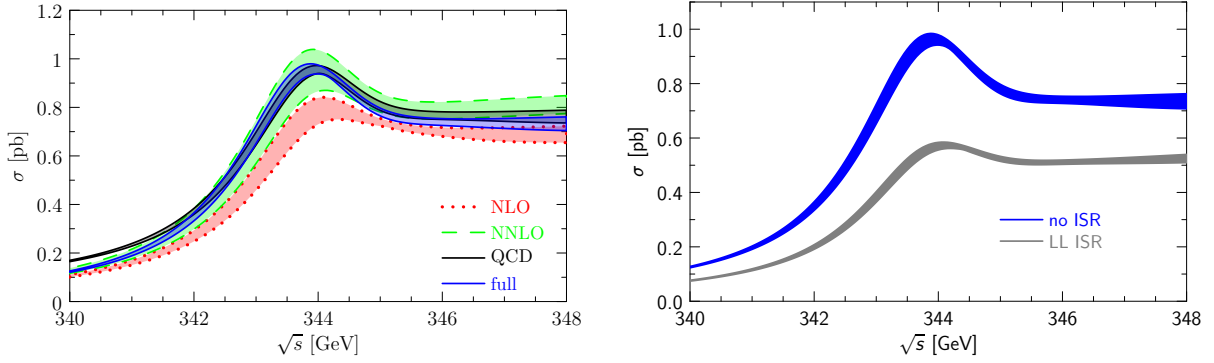


Fig. B.11.2: Total cross-section for the process $e^+e^- \rightarrow t\bar{t}$ at various orders in perturbation theory. Left: Cross-section without ISR from NLO to NNNLO with the pure NNNLO QCD result as comparison. Right: Effect of ISR on the cross-section.

cross-section. A detailed account of the NNLO calculation including the arrangement of pole cancellations is given in Ref. [16].

11.3.3 Initial-state radiation

Formally, photonic corrections in the initial state are suppressed by one order in α and therefore contribute at NNLO according to our power counting. However, it is well-known that these corrections are enhanced by logarithms of m_t over m_e , which have to be resummed to all orders. The resummed cross-section is given by [23, 24]

$$\sigma(s) = \int_0^1 dx_1 \int_0^1 dx_2 \Gamma_{ee}^{\text{LL}}(x_1) \Gamma_{ee}^{\text{LL}}(x_2) \hat{\sigma}(x_1 x_2 s) + \sigma_{\text{const}}^{\text{ISR}}(s), \quad (11.4)$$

where $\Gamma_{ee}^{\text{LL}}(x)$ is a leading logarithmic structure function, $\hat{\sigma}$ is the ‘partonic’ cross-section without ISR resummation and $\sigma_{\text{const}}^{\text{ISR}}$ accounts for the non-logarithmic NNLO contribution.

11.4 Cross-section predictions

The formulae for the cross-section can be evaluated numerically with the code `QQbar_threshold` [25], which includes all aforementioned corrections. Figure B.11.2 shows the behaviour of the total cross-section near threshold for a top quark mass of $m_t(20 \text{ GeV}) = 171.5 \text{ GeV}$ in the potential-subtracted scheme [26] and input parameters $\Gamma_t = 1.33 \text{ GeV}$, $m_H = 125 \text{ GeV}$, $\alpha_s(m_Z) = 0.1177$, $\alpha(m_Z) = 1/128.944$. The uncertainty bands originate from a variation of the renormalization scale between 50 and 350 GeV.

Figure B.11.3 shows the effect of changing various parameters. The variation suggests that it should be possible to extract the top quark width and mass in the potential-subtracted scheme with an uncertainty of better than 100 MeV. The sensitivity to the top Yukawa coupling and the strong coupling is less pronounced and there is a considerable degeneracy between the two parameters. A precise knowledge of the strong coupling constant from other sources will be crucial to meaningfully constrain the Yukawa coupling. In any case, a dedicated experimental analysis will be needed to determine the exact precision with which the various top quark properties can be extracted from a measurement of the cross-section.

Acknowledgements

I thank the CERN Theory Department for their hospitality and support during the workshop.

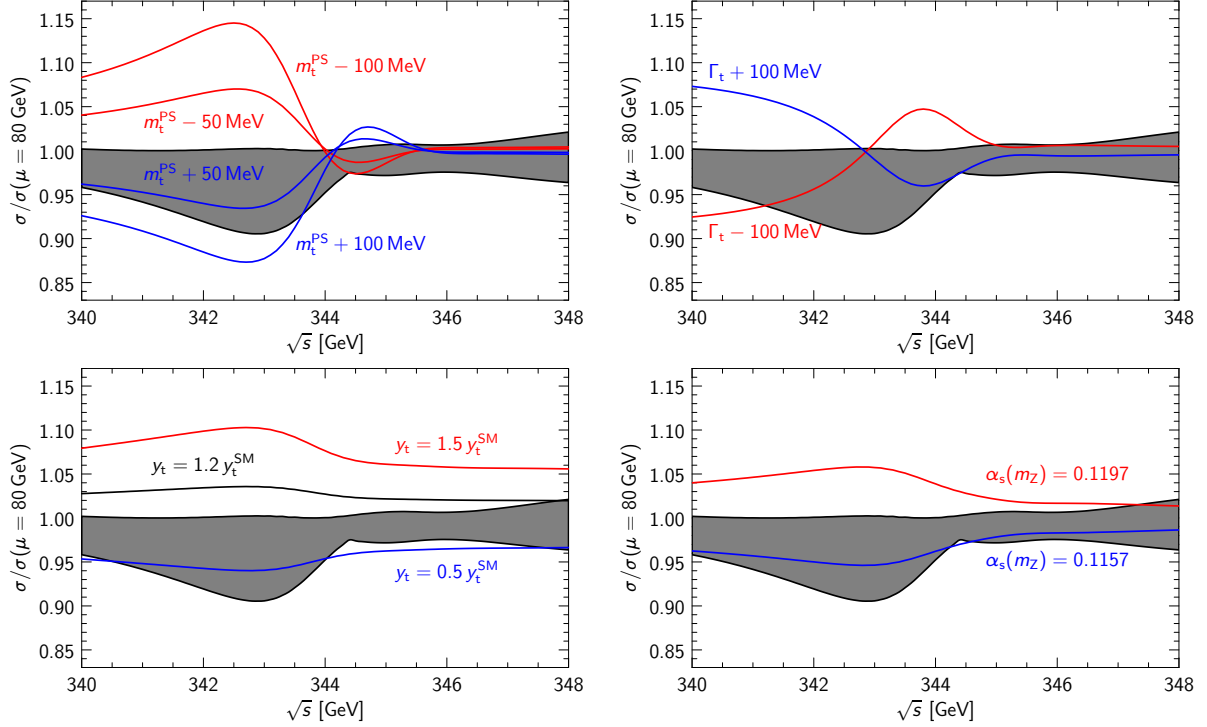


Fig. B.11.3: Sensitivity of the cross-section to parameter variation. Top left: Variation of the top quark mass by up to ± 100 MeV. Top right: Variation of the top quark width by up ± 100 MeV. Bottom left: Variation of the top Yukawa coupling. Bottom right: Variation of the strong coupling constant.

References

- [1] K. Seidel *et al.*, *Eur. Phys. J.* **C73** (2013) 2530. [arXiv:1303.3758](#), [doi:10.1140/epjc/s10052-013-2530-7](#)
- [2] F. Simon, *PoS ICHEP2016* (2017) 872. [arXiv:1611.03399](#), [doi:10.22323/1.282.0872](#)
- [3] A. Pineda and J. Soto, *Nucl. Phys. Proc. Suppl.* **64** (1998) 428. [arXiv:hep-ph/9707481](#), [doi:10.1016/S0920-5632\(97\)01102-X](#)
- [4] M. Beneke and V.A. Smirnov, *Nucl. Phys.* **B522** (1998) 321. [arXiv:hep-ph/9711391](#), [doi:10.1016/S0550-3213\(98\)00138-2](#)
- [5] N. Brambilla *et al.*, *Nucl. Phys.* **B566** (2000) 275. [arXiv:hep-ph/9907240](#), [doi:10.1016/S0550-3213\(99\)00693-8](#)
- [6] M. Beneke *et al.*, *Phys. Rev. Lett.* **93** (2004) 011602. [arXiv:hep-ph/0312331](#), [doi:10.1103/PhysRevLett.93.011602](#)
- [7] M. Beneke *et al.*, *Nucl. Phys.* **B686** (2004) 205. [arXiv:hep-ph/0401002](#), [doi:10.1016/j.nuclphysb.2004.03.016](#)
- [8] D. Eiras and M. Steinhauser, *Nucl. Phys.* **B757** (2006) 197. [arXiv:hep-ph/0605227](#), [doi:10.1016/j.nuclphysb.2006.09.010](#)
- [9] M. Beneke *et al.*, *Nucl. Phys.* **B880** (2014) 414. [arXiv:1312.4792](#), [doi:10.1016/j.nuclphysb.2014.01.015](#)

- [10] P. Marquard *et al.*, *Phys. Rev.* **D89** (2014) 034027. [arXiv:1401.3004](#),
[doi:10.1103/PhysRevD.89.034027](#)
- [11] M. Beneke *et al.*, *Nucl. Phys.* **B899** (2015) 180. [arXiv:1506.06865](#),
[doi:10.1016/j.nuclphysb.2015.07.034](#)
- [12] B. Grzadkowski *et al.*, *Nucl. Phys.* **B281** (1987) 18. [doi:10.1016/0550-3213\(87\)90245-8](#)
- [13] R.J. Guth and J.H. Kühn, *Nucl. Phys.* **B368** (1992) 38.
[doi:10.1016/0550-3213\(92\)90196-I](#)
- [14] A.H. Hoang and C.J. Reisser, *Phys. Rev.* **D71** (2005) 074022. [arXiv:hep-ph/0412258](#),
[doi:10.1103/PhysRevD.71.074022](#)
- [15] A.H. Hoang and C.J. Reisser, *Phys. Rev.* **D74** (2006) 034002. [arXiv:hep-ph/0604104](#),
[doi:10.1103/PhysRevD.74.034002](#)
- [16] M. Beneke *et al.*, *JHEP* **02** (2018) 125. [arXiv:1711.10429](#),
[doi:10.1007/JHEP02\(2018\)125](#)
- [17] C. Anzai *et al.*, *Phys. Rev. Lett.* **104** (2010) 112003. [arXiv:0911.4335](#), [doi:10.1103/PhysRevLett.104.112003](#)
- [18] A.V. Smirnov *et al.*, *Phys. Rev. Lett.* **104** (2010) 112002. [arXiv:0911.4742](#), [doi:10.1103/PhysRevLett.104.112002](#)
- [19] R.N. Lee *et al.*, *Phys. Rev.* **D94** (2016) 054029. [arXiv:1608.02603](#), [doi:10.1103/PhysRevD.94.054029](#)
- [20] M. Beneke *et al.*, *Phys. Rev. Lett.* **115** (2015) 192001. [arXiv:1506.06864](#),
[doi:10.1103/PhysRevLett.115.192001](#)
- [21] A.A. Penin and A.A. Pivovarov, *Phys. At. Nucl.* **64** (2001) 275, [*Yad. Fiz.* **64** (2001) 323].
[arXiv:hep-ph/9904278](#), [doi:10.1134/1.1349450](#)
- [22] M. Beneke *et al.*, *Nucl. Phys.* **B840** (2010) 186. [arXiv:1004.2188](#),
[doi:10.1016/j.nuclphysb.2010.07.006](#)
- [23] E.A. Kuraev and V.S. Fadin, *Sov. J. Nucl. Phys.* **41** (1985) 466 [*Yad. Fiz.* **41** (1985) 733].
- [24] V.S. Fadin and V.A. Khoze, *JETP Lett.* **46** (1987) 525 [*Pisma Zh. Eksp. Teor. Fiz.* **46** (1987) 417]. http://www.jetpletters.ac.ru/ps/1234/article_18631.shtml
- [25] M. Beneke *et al.*, *Comput. Phys. Commun.* **209** (2016) 96. [arXiv:1605.03010](#),
[doi:10.1016/j.cpc.2016.07.026](#)
- [26] M. Beneke, *Phys. Lett.* **B434** (1998) 115. [arXiv:hep-ph/9804241](#),
[doi:10.1016/S0370-2693\(98\)00741-2](#)